doi: 10.15407/ujpe60.08.0708

K.V. CHEREVKO,[1] L.L. JENKOVSZKY,[2] V.M. SYSOEV,[1] FENG-SHOU ZHANG [3, 4, 5]

[1] Faculty of Physics, Taras Shevchenko National University of Kyiv
(4, Academician Glushkov Ave., Kyiv 03022, Ukraine; e-mail: k.cherevko@univ.kiev.ua)
[2] Bogolyubov Institute for Theoretical Physics, Nat. Acad. of Sci. of Ukraine
(Metrolohichna Str. 14-b, Kyiv, 03680, Ukraine; e-mail: jenk@bitp.kiev.ua)
[3] College of Nuclear Science and Technology, Beijing Normal University
(Beijing 100875, China)
[4] Beijing Radiation Center
(Beijing 100875, China)
[5] Center of Theoretical Nuclear Physics, National Laboratory of Heavy Ion Accelerator of Lanzhou
(Lanzhou 730000, China; e-mail: fszhang@bnu.edu.cn)

PACS 05.70.-a, 21.65.-f, 25.70.-z, 25.75.-q

COMMON APPROACHES IN DESCRIPTION OF ORDINARY LIQUIDS AND HADRONIC MATTER

This work is an attempt to give a brief overview of the implementation of the statistical thermodynamics to hadronic matter. The possibility to use the hydrodynamic approach for developing the physical model of the formation of exotic structures in the head-on intermediate-energy heavy ion collisions is discussed. That approach is shown to be able to provide simple analytical expressions describing each step of the collision process. This allows for extracting the data concerning nuclear matter properties (surface tension, compressibility, etc.) from the properties of observed fragments. The advantages of the thermodynamic analysis of phase trajectories of the system in heavy ion collisions are discussed. Within the thermodynamic approach, the method to evaluate the curvature correction to the surface tension from the nuclear matter equation of state is described. The possibility to use statistical thermodynamics in the studies of hadronic matter and quantum liquids is discussed.

K e y w o r d s: heavy ion collisions, equation of state, hydrodynamic instability, phase diagram, Tolman length, thermodynamics, Skyrme parametrization.

1. Introduction

The study of the properties of hadronic matter and the phase transitions in it has been the subject of many studies both theoretical and experimental in recent decades. Such an interest is explained both by the applied importance of results for the energy production industry, radiation medicine and by their fundamental importance, because the many-body systems, in which the excitation energy is thermally distributed among many particles and in which there exist long-range Coulomb and short-range forces, up to now have no satisfactory description. The description of nuclear matter (NM) within statistical thermodynamics adopted in the recent decades is very similar to that for ordinary liquids [1–4]. The physical reason for that is the similarity between the molecular forces and nuclear-nuclear interactions in respect to their dependence on the distance. Notwithstanding the tremendous difference in the energy and space scales, the nuclear and van der Waals forces represent a very similar behavior. In both cases, the attraction between particles is replaced by their repulsion at a small interaction range. J.D. van der Waals suggested

his famous equation in 1873. A hundred years later, his finding was fruitfully used to describe the properties of the nuclear matter unknown to the nineteenth century scientists. It is quite natural to expect that, when investigating both ordinary liquids and nuclear matter, it is reasonable to use similar fundamental concepts of the modern thermodynamics, statistical physics, phase transitions theory, and the liquid state theory accounting for the quantum nature of nuclear matter.

Among all the studies of nuclear systems, of high importance are those devoted to the processes observed in heavy ion collisions (HIC). Such studies are valuable from the fundamental point of view, as it is the only available experimental method (under the Earth conditions) to obtain data about the nuclear matter at extreme temperatures and densities. As for the applied importance, the results are needed to proceed in developing the new technologies of the nuclear waste utilization, which is an up-to-date task accounting for the rapid development of the nuclear energy production industry. The other important applications can be found in medical physics and biophysics. When the beams of high-energy ions pass through the matter, they leave the trace of the fragments produced in the collision, causing the changes in structures and thermodynamic properties of biological objects and liquids. Therefore, the clear understanding of the fragments formation mechanisms can help in biophysical studies and in developing the new technologies in the medical physics.

Nowadays, it could be seen that, in the field of studies devoted to the HIC, the progress in experimental researches is much faster than in theoretical ones. Unfortunately, there are yet no complete theories of such important phenomenon as the nuclear multifragmentation, no satisfactory equation of state (EOS) for hadronic matter, and no clear understanding of phase transitions in nuclear matter. Therefore, the progress in the theory able to describe the basic thermodynamic and structural properties of hadronic matter, phase transitions in it, and behavior of hot nuclei with high excitation energies stands among the most important problems in modern physics.

To recall the stage, we would like to present a brief overview of the problems that exist in hadronic matter physics and can be studied with the help of statistical thermodynamics and the theory of phase transitions well developed for ordinary liquids.

1.1. Nuclear matter equation of state

The knowledge of the EOS of nuclear matter is one of the fundamental goals in nuclear physics, which has not yet been achieved [5–9]. It should describe the fundamental properties of NM

$$P = P(\rho, T, \delta), \tag{1}$$

where P is the pressure, ρ is the density, and δ is an asymmetry parameter, at any point of the phase diagram of NM (Fig. 1). The EOS of NM is an important ingredient in studying the properties of nuclei at and far from stability, studying the structures and the evolution of compact astrophysical objects such as neutron stars and core-collapse supernovae, applied nuclear physics, *etc.* The saturation point of EOS, i.e., the energy as a function of the matter density, for the symmetric NM (SNM) at zero temperature ($T = 0$), is well determined from the ground-state properties of nuclei, such as binding energies and central matter densities, by extrapolation to infinite NM [11]. At the same time, one can find the vast majority of different parametrizations and different theoretical models that were built in attempt to describe the NM and finite nuclei in a wide range of the external parameters. All of them were built for the case of special assumptions and are lacking a predictive power [12].

The things go even worth, when one changes to the asymmetric NM and the pure neutron matter. Existing models give different results for the symmetry energy of asymmetric NM [13], its slope, and magnitude

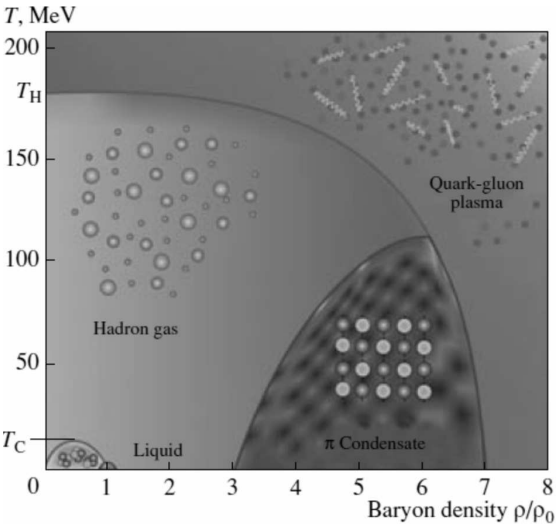

Fig. 1. Phase diagram of NM [10]

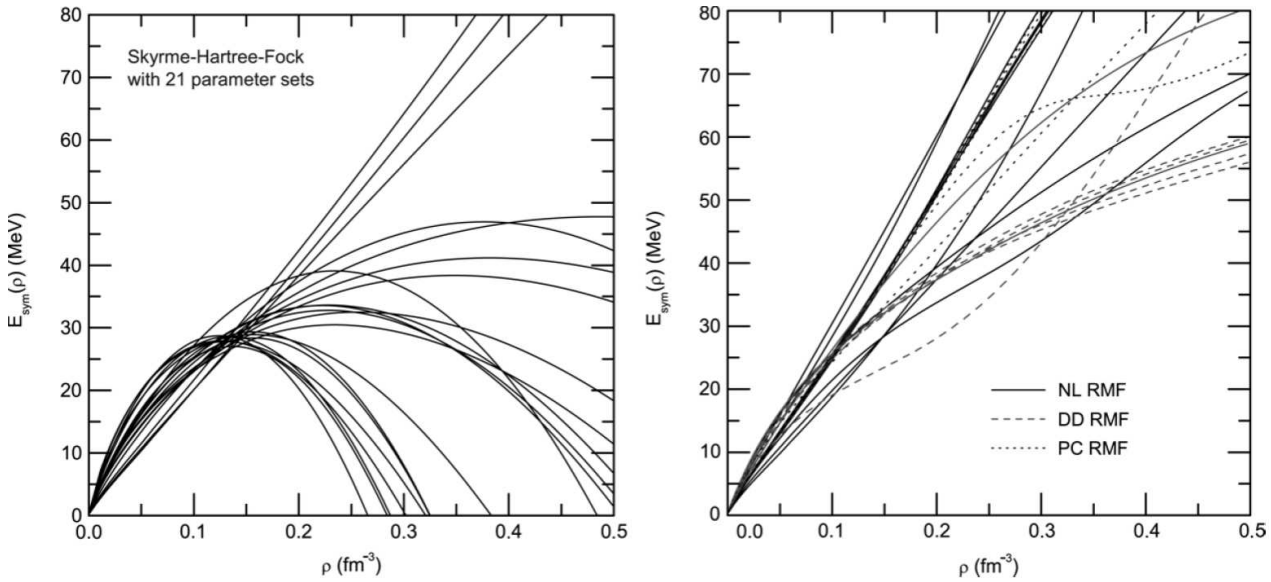

Fig. 2. Left window: Density dependence of the nuclear symmetry energy $E_{sym}(\rho)$ from SHF with 21 sets of Skyrme interaction parameters [15]. Right window: Same as left panel from the RMF model for the parameter sets NL1, NL2, NL3, NL-SH, TM1, PK1, FSU-Gold, HA, NLρ, and NL$\rho\delta$ in the nonlinear RMF model (solid curves); TW99, DD-ME1, DD-ME2, PKDD, DD, DD-F, and DDRH-corr in the density-dependent RMF model (dashed curves); and PC-F1, PC-F2, PC-F3, PC-F4, PC-LA, and FKVW in the point-coupling RMF model (dotted curves) [16]

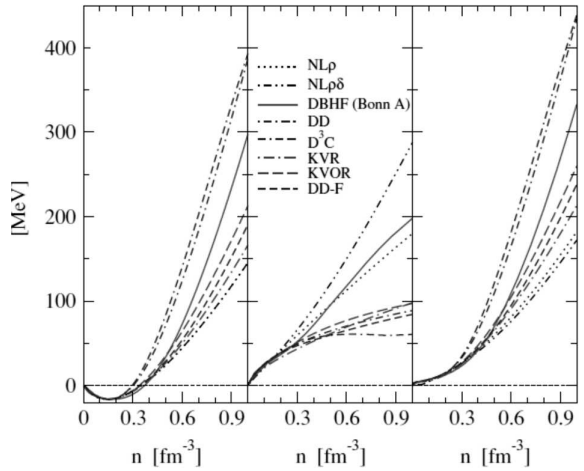

Fig. 3. Energy per nucleon in SNM $E_0(n)$ (left panel), the symmetry energy $E_s(n)$ (middle panel), and the energy per nucleon in a nonsymmetric NM (NNM) (B-equilibrated and charge neutral) for different models (right panel) [17]

at the saturation density and, the experimental constraints are quite wide [14]. It should be noted that the symmetry energy behavior is very different for different EOS parametrizations [9] in the high- and low-density regions (Fig. 2).

The similar uncertainty is observed for a symmetric NM (SNM) in the high-density region (Fig. 3).

Nowadays, extracting the information on the nuclear EOS, in particular at high baryon densities, is restricted to observations of astrophysical compact objects and studies of hot nuclear systems created in high-energy proton-induced reactions or in intermediate and relativistic energy heavy-ion collisions (HIC).

Therefore, HIC can shed light on what are nuclei made of and explain the properties of the matter that form the nuclei. Such experiments can be treated as a kind of materials science similar to the P-V-T studies in the physics of ordinary liquids. Hence, it is quite natural to apply the well-developed theories of ordinary liquids to the description of HIC. Understanding the behavior of NM in the HIC is of great relevance either for theoretical nuclear physics or for nuclear astrophysics, when studying the supernova explosions and the properties of neutron stars [18–20].

2. Heavy Ion Collisions

The idea of HIC experiments is to collide two nucleus or light particles with nuclei at a high enough energy to break them into pieces. Introducing then an ap-

propriate model of the process involved, it should be possible to extract some data on NM properties and its behavior at high densities and temperatures. The basic mechanisms of the formation of fragments in the HIC experiments are the following [21]:

• spallation, when only one heavy fragment with its mass close to the target mass is formed ($m = 1$);

• fission that goes usually with the two heavy fragments produced with masses in the interval around half the target mass $A \sim \frac{A_T}{2}$;

• multifragmentation that is the process which leads to the formation of several fragments with intermediate masses. Usually with $A < 50$.

The last one is especially important in studies of the NM EOS. Disintegration, when a bigger nucleus breaks into one or several nuclei and some nucleons, is one of the two basic mechanisms in the Nature, by which a nuclei can be formed. The appropriate way to study this phenomenon is the experiment with proton-nucleus and nucleus-nucleus collisions. When such a collision is observed at a high enough energy (higher than the threshold value $E_{\rm th} \sim 2$–4 MeV/nucleon [22]), there is a high probability of the production of intermediate-mass fragments [23,24]. The nature of the production of intermediate-mass fragments in such experiments is of great interest for the consequent understanding of the NM properties and for the progress in the studies of nuclear EOS [24–29]. Thus, HIC have been intensively studied in the last years [25, 30]. It should be noted that, in a composite system formed in the collision process from the projectile and target nuclei, nuclear matter can be highly compressed and be at high temperatures during the early stage of the reaction. At the time of the formation of intermediate-mass fragments with $3 \leq Z \leq 20$, their characteristic properties such as the excitation energy and isotopic distributions are governed by the characteristics of the break-up source such as the temperature, density, and N/Z ratio. Therefore, intermediate-mass fragments may provide a unique probe to study the reaction mechanism and hot nuclear matter properties [31].

At the same time, in order to have the complete picture of the situation in a field, one should bear in mind that the colliding system is over a large time span of the reaction out of global and even local equilibrium [27]. That means the presence of the non-equilibrium effects all over the compression phase, where one essentially intends to study the NM EOS. The other important challenge is that the heavy ion collision experiments are inclusive and will remain so in the foreseeable future. That means missing some information about the physical processes going on in the system. Only the degree of inclusiveness may change if more sophisticated counter arrays are introduced [21].

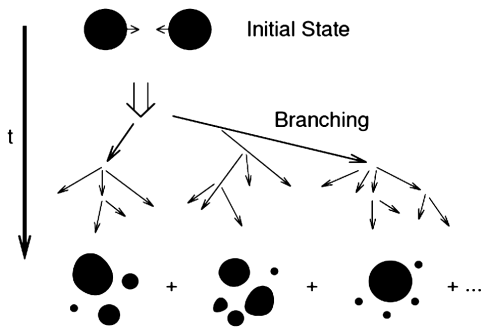

Fig. 4. Schematic picture of a fragmentation reaction, in which a given initial channel may develop into many different fragmentation channels during the dynamical evolution [37]

During the last decades, a wealth of data have been accumulated about the multifragmentation phenomenon in proton-nucleus and nucleus-nucleus collisions [10, 21, 32, 33]. Different models (statistical [19, 34], percolation [35]) and different mechanisms (liquid-gas phase transitions, spinodal decomposition, sequential evaporation from the expanding-emitting source, *etc.* [36]) are being used for explaining the existing data. As for the initial highly non-equilibrium stage, the most common approach is using the transport models for its adequate description. One of the important points in that case is allowing the model for the possibility for the occurrence of dynamical bifurcations (Fig. 4), as it is a non-linear process [37].

There exist a number of different transport models that have been developed till now. Among them are intranuclear cascade calculations, time-dependent Hartee–Fock model, Boltzmann-type kinetic equations based on hadronic non-equilibrium quantum transport field theory, molecular dynamics methods (MD, QMD, AMD, FMD), nuclear fluid dynamics calculations, *etc.* The detailed analysis can be found elsewhere (e.g., [27,37–40]), but, summarizing all pros and cons, it is possible to conclude that although much progress has been made over the past couple of decades, we are still far from having models that are formally well founded, practically applicable, and sufficiently realistic to be quantitatively useful. The description of nuclear fragmentation dynamics requires

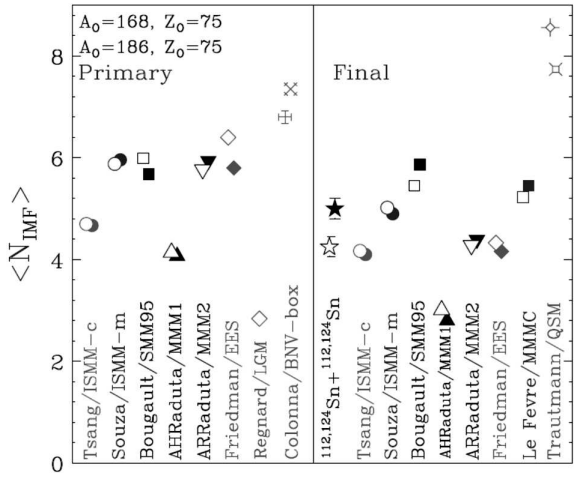

Fig. 5. Mean IMF multiplicity obtained from different statistical models. The open and solid stars on the right panel are data from the central collisions of ^{112}Sn + ^{112}Sn and ^{124}Sn + ^{124}Sn systems at $E = A = 50$ MeV [41]

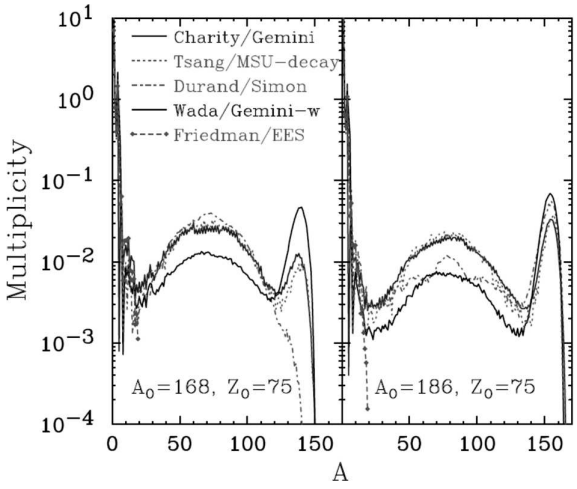

Fig. 6. Predicted mass distributions from five evaporation codes for neutron-deficient system 1 (left panel) and neutron-rich system 2 (right panel) [41]

that the proper account for the basic quantal nature of the system be taken [37].

Similar situation is observed for the later stages of the collision. One of the considerable problems is that the time needed for the equilibration and the transition to the statistical description is still under debate. The other difficulty to be overcome is that most statistical multifragmentation codes have been developed to describe specific sets of data and nearly all of them have different assumptions. They are not equivalent [41]. Basically, two main sets of models are used to describe the final stages of the reaction that are the multifragmentation models and the evaporation models. From the data available in the literature [41], one can see (Figs. 5 and 6) that the overall behavior of the systems shows a similarity among models suggesting some predictive power as for system's behavior in the multifragmentation phenomena and allowing for suggesting physical processes responsible for the formation of fragments. At the same time, the behaviors of single observables differ from model to model suggesting some limitations on their applicability in treating the experimental results.

In spite of a long history and a high number of different approaches used, there is still a number of problems left that have no explanation. For example, the models involving a phase transition have the strong position based on the recent works dealing with the bimodality [42]. But, in the same time, their justification is quite questionable. They are insensitive to many initial parameters [21], when it is known for ordinary liquids that the phase transition is usually the quantity difficult to be prepared. The most successful models in describing the observed fragment mass distribution nowadays are the statistical equilibrium models [43,44] that try to reduce the intractable problem of a time-dependent highly correlated interacting many-body fermion system to the much simpler picture of a system of non-interacting clusters [45]. First based on Bevalac's results, they were used for intermediate energies of HIC with many substantial variations [28]. In the same time, such models have a number of difficulties [21, 43]. The question with the equilibrium at a low freeze-out density that lies in the basis of such theories is not confirmed by some microscopic approaches. There are evidences of only a small part of the system being heated [21, 44]. The other problem concerns with the predicted kinetic energy of fragments, being lower than the temperature of the gas of fragments [44], *etc.*

Therefore, the determination of the mechanism responsible for the multifragmentation phenomenon and able to solve the existing problems in natural way is of particular interest as this issue has not been settled up to now.

2.1. Thermodynamics of heavy ion collisions

The interest to the intermediate-energy collisions is triggered by a fact that the multifragmentation is

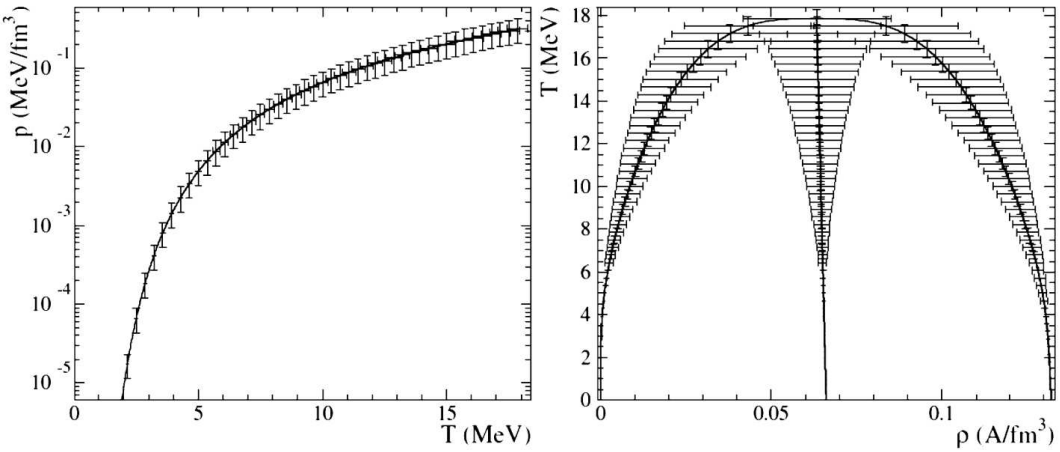

Fig. 7. Left: the pressure-temperature coexistence curve for bulk nuclear matter. Right: the temperature–density coexistence curve for bulk nuclear matter. Errors are shown for selected points to give an idea of the error on the entire coexistence curve [46]

claimed to be connected with a phase transition in NM [46]. Such an assumption comes from the thermodynamic analysis of the coexistence curve in NM (Fig. 7) based on the intermediate HIC data. In that case, the Fisher droplet model is widely used due to the fact that the distribution of fragments can be described by Fisher's well-known formulae for the droplet mass distribution [47, 48]

$$\frac{dP}{dM} \sim M^{-\alpha}, \tag{2}$$

where P is the fragment formation probability, M is the mass, and α is the critical exponent. In that case, the basic principles of the analysis are absolutely the same as in the physics of ordinary liquids. The description of the formation of clusters is based [49] on the Gibbs balance equation for the free energy G:

$$\Delta G = \Delta E - T\Delta S + P\Delta V, \tag{3}$$

where ΔE and ΔS are the energy and entropy costs of the formation of a cluster, respectively, P is the pressure and ΔV is a change in the volume owing to the formation of a cluster. Within such approach, it appears next to be possible to use the classical Guggenheim relation for the coexistence curve [50]:

$$\frac{\rho_{l,v}}{\rho_c} = 1 + b_1\left(1 - \frac{T}{T_c}\right) \pm b_2\left(1 - \frac{T}{T_c}\right)^{\beta}, \tag{4}$$

where b_1, b_2 are the parameters and $\beta = \frac{(\tau-2)}{\sigma}$ [48] is the critical exponent. Equation (4) together with the experimental vapor branch of the coexistence curve [49]

$$\frac{\rho}{\rho_c} = \frac{\sum An_A(T)}{\sum An_A(T_c)}, \tag{5}$$

allow constructing the complete coexistence curve of nuclear matter (e.g., see Fig. 7). Within this approach, the modern theory of phase transitions together with the thermodynamics allow estimating the critical temperature in infinite NM and a finite nucleus. That can give, in turn, a deep insight into the properties of NM and can be of great importance for developing the proper NM EOS. Quite promising is the thermodynamic analysis of the phase trajectories of systems formed in HIC. Recently, there appeared a work devoted to the study of different possible phase trajectories of the excited nuclear system at the $P-V$ plane [51]. It was aimed to get a qualitative picture of the phenomenon considering the boundness of the system and the existing laws, which describe the behavior of the ordinary liquids in the metastable and spinodal states [52]. Assuming the system before the collision to be at point L of the phase diagram (Fig. 8), the different scenarios of system's evolution were studied.

Evolution of the system crucially depends on the excitation energy, mass number, and energy release conditions. This position suggests two different groups of phase trajectories, namely: the single-phase transition (marked with the dashed line) and two-phase transitions (marked with the solid line). It is

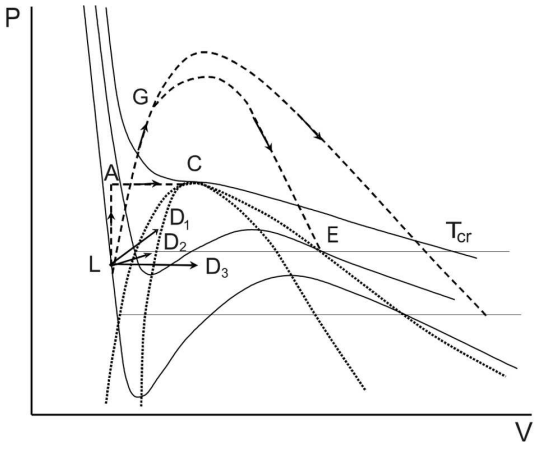

Fig. 8. Possible phase trajectories of a nuclear system in the proton-induced multifragmentation phenomenon

obvious that there could be a mixture of two decay channels, when different parts of the system are found in different areas of the phase diagram. Thus, one may say that the nuclear multifragmentation is a nonlinear phenomenon, which means that the qualitative picture is different depending on system's parameters. The thermodynamic analysis conducted in the work has shown that not all of the mechanisms could be realized in nuclear systems because of their size. Some mechanisms does not meet the requirements for the time needed for the process. Summing up all pros and cons of different decay channels and qualitative characteristics, it was suggested that the spinodal decomposition could not be responsible for the multifragmentation phenomena because of the system size. That fact can be explained from Cahn's theory of separation by the spinodal decomposition [53]. In that theory, changes in the free energy read

$$\Delta F = \int \left[\frac{1}{2} \left(\frac{\partial^2 f}{\partial c^2} (c - c_0)^2 \right) + K(\nabla c)^2 \right] dV, \qquad (6)$$

where f is the free-energy density of a homogeneous material with composition c, $K(\nabla c)^2$ is the additional free energy density if the material is in a gradient in the composition. Therefore, the system is unstable relative to the Fourier components with $\beta < \beta_c = \left(-\frac{\partial^2 f / \partial c^2}{2K} \right)^{1/2}$ or sufficiently large wavelengths, as this decreases the free energy, when the system is in the unstable region. This result shows that, for the smaller wavelengths, there is no decrease in system's free energy, and there is no sign change in the diffusion coefficients. Therefore, for a small enough system, the spinodal behavior cannot be justified. As for the most appropriate decay channel, it appeared to be the mechanical breakdown of the shell in a single-phase process that may be followed by the metastable boiling. Although, there also could be a mechanism based on the metastable boiling of the inner part of the system. The suggested thermodynamic analysis allowed for a simple qualitative picture of the phenomena. At the same time, some further quantitative estimations based on the combination of macroscopic and microscopic theories, as well as on computer simulation results, are needed.

There exist quite a lot of other examples (e.g., [54] and references therein) of the successful implementation of statistical thermodynamics approaches to quantum systems and nuclear matter, in particular. This suggests the thermodynamics to be an important ingredient in the nuclear matter studies.

2.2. Exotic topologies in the intermediate energy collisions. Hydrodynamic approaches

The hydrodynamic description of nuclear matter dates back to the 1980s (see, e.g., [55, 56]) and is now widely used for the high energy HIC. In some pioneer works [57], the possibility to use the hydrodynamic description in the lower-energy limit was confirmed, by basing on the analysis of the nucleon mean free path that was defined as $\lambda = 1.4 \frac{\rho_0}{\rho}$fm. Later on, quite a lot works addressed the problem of a nucleon mean free path and the evaluation of the in-medium nucleon cross section, with the Pauli blocking being considered [58–60]. Still, the results found in some more recent publications [61] with the parametrized in-medium nucleon-nucleon cross sections from the Dirac–Brueckner approach based on the Bonn-A potential give the values $\lambda \sim 1.4$ fm and $\lambda \sim 1.3$ fm for $\rho/\rho_0 = 1$ and $\rho/\rho_0 = 1.5$, respectively, at $E = 50$ MeV/nucleon. Those results confirm well the argumentation in [57]. Despite that, the hydrodynamic description of the HIC at intermediate and low energies has been the subject of only few theoretical studies [62]. During the last decades in a number of works, the possibility of the formation of toroidal (Fig. 9) and bubble (Fig. 10) structures in the head-on HIC was studied extensively with the help of microscopic transport models [63, 64]. Within the Boltzmann–Uehling–Uhlenbeck (BUU) model, it was shown that,

at the energy interval 60–75 MeV/A, the different exotic topologies of the formed objects can be observed, depending on the stiffness of the nuclear mater EOS. Main peculiarities observed in the qualitative picture, which comes from the Boltzmann–Uehling–Uhlenbeck calculations and the available experiments [63, 64], are the fact that the expanding velocity of the outer surface of the system is much smaller than the expanding velocity of the inner surface, simultaneous breakup with few fragments of similar masses and low kinetic energies and with the angular distribution of fragments that is almost isotropic in the case of soft EOS (the incompressibility at saturation density $K_0 = 200$ MeV), and the presence of fragments in the plane perpendicular to the beam direction for the stiff EOS (the incompressibility at the saturation density $K_0 = 380$ MeV). For some time, the experimental results were not able to confirm the occurrence of the predicted geometries [65]. But, later on, the signatures of the "doughnut"–like structures with the production of similar-size intermediate-mass fragments were observed in central HIC [66] and again confirmed by transport models [61]. Unfortunately the calculations with transport theories used for the phenomena in focus are not able to give reliable information on multiparticle observables at the late stage of the process due to the fact that they do not include multiparticle correlations and fluctuations [64]. In some works [63, 67], the Rayleigh–Taylor mechanism was suggested to be responsible for the formation of fragments, when the exotic topologies were explained with the help of shock waves. Such type of structures is also somewhat similar to those studied theoretically from another approach [68]. Different shapes observed in the experiment may yield the valuable information about the nuclear incompressibility, which is a key parameter of the nuclear EOS, as well as the information regarding the surface tension and NM viscosity. The possibility for different shock wave mechanisms to be involved into the process can also give an extra link in between the Boltzmann-like transport theory and the hydrodynamic approach. Recently, it was shown [69] that the observed qualitative picture has much in common with the collisions of high-speed ordinary droplets [70–72]. For the latter in the certain energy range, the formation of "doughnut"–like structures with the following fragmentation into several secondary drops of approximately equal masses is observed [73], which has much in common with the nuclear case [64]. In a recent work [69], the system of two identical heavy nuclei (e.g. ^{93}Nb + ^{93}Nb) involved in a head-on collision was considered. The symmetry of the system allowed the simplification of the model by changing to the collision of a spherical nuclei of radius R and density ρ_0 with a rigid wall that moved

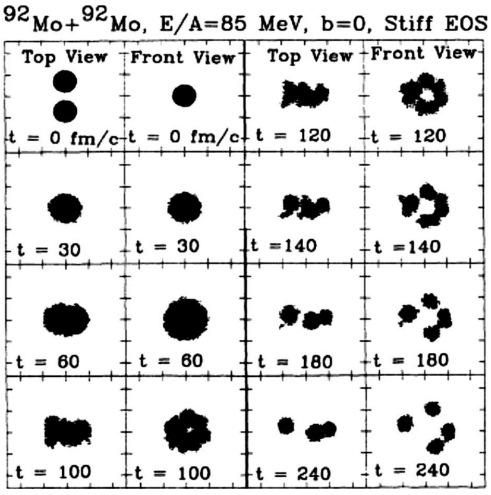

Fig. 9. BUU calculations with the stiff EOS for ^{92}Mo + ^{92}Mo collisions at $E/A = 85$ MeV, $b = 0$. Only the areas with densities $\rho > 0.1\rho_0$ are shown. The scales between neighboring ticks are 10 fm [64]

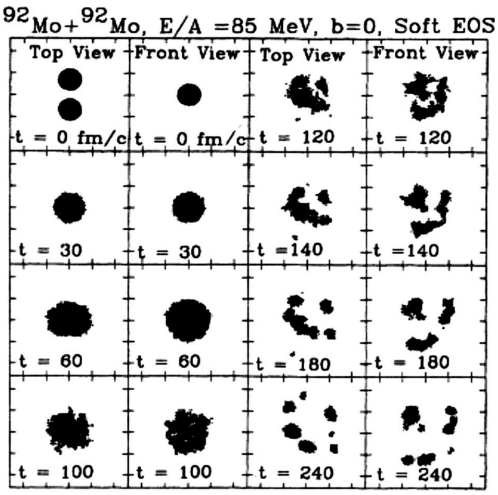

Fig. 10. BUU calculations with the soft EOS for ^{92}Mo + + ^{92}Mo collisions at $E/A = 85$ MeV, $b = 0$. Only the areas with densities $\rho > 0.1\rho_0$ are shown. The scales between neighboring ticks are 10 fm [64]

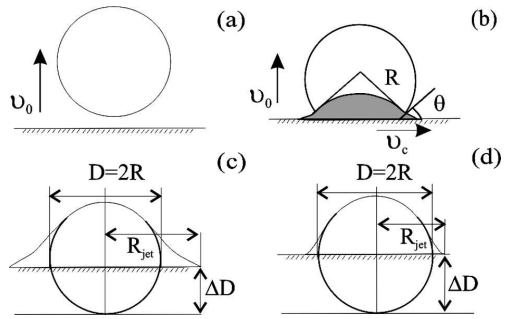

Fig. 11. Different stages of the evolution: symmetry plane impacting the nuclei *a*; lateral jetting, when the shockwave velocity becomes equal to the contact edge velocity *b*. Compressed zone is shown in grey. The geometry of the system in the case of "stiff" EOS ($K = 380$ MeV) *c*; geometry in the case of "soft" EOS ($K = 200$ MeV) *d*

toward it with the velocity υ_0 (Fig. 11, *a*). The slip boundary condition was applied on the wall surface to account for the difference in a viscous behavior.

From the analysis of the recent theoretical and experimental results for the collisions of liquid droplets [74–76] together with the BUU [64] and nuclear fluid dynamics (NFD) [40] results for HIC, it is suggested that there should be four distinct stages of the collision [Fig. 11]. Among them are the violent stage at the beginning of the process, when the highly compressed zone is formed, and the second stage that is characterized by the lateral jetting and lasts till the shock wave from collision plane reaches the boundary of the nuclei. During those two stages, the final topology of the system is fully defined. At the later times, the system goes through the third stage corresponding to the expansion process and finally comes to the last stage, when the fragmentation takes place. The main quantitative estimations within the suggested model and their comparison with the BUU calculations and experimental data are presented in Table.

Quantitative characteristics of the process for the ^{93}Nb + ^{93}Nb system at 60 MeV/nucleon with "stiff" EOS ($K = 380$ MeV)

	[69]	[63, 64]	[66]
Reaction time τ_3, fm/c	118	120–160	
Maximum density ρ/ρ_0	1.6	∼1.5	
Spreading size $\frac{R_\perp^{\max}}{R}$	2.6	∼2	
Rim radius at τ_3, fm	1.9		
Number of similar mass IMF	5.6	3–6	4–6

One can see that the above model slightly overestimates the spreading size and underestimates the reaction time. This probably comes from the approximations used in the model. For example, accounting for the viscous dissipation and changing to the Navier–Stokes equations, as well as accounting for the changes in the surface tension coefficient due to the temperature increase, can influence both of the above values. The model doesn't give the strict results, but rather provides a picture of the involved physical processes as clear as possible. For such a model with no adjustable parameters, the results for the maximum density and overall timescale of the process are in good correspondence with the BUU calculations. It is also worth mentioning that the result for the number of fragments of similar masses is in good correspondence both with the experiment and the BUU calculations. Such results show that the hydrodynamic description based on the laws developed for ordinary liquids seems to explain the overall behavior of the nuclear systems in the head-on HIC in focus and allows a simple physical picture of the formation of exotic structures.

One can conclude that the combination of the hydrodynamic approach together with the transport theory calculations can reveal the physical nature of the phenomena observed in HIC and give possibility to proceed with extracting the data on the NM properties from the HIC at different energies.

3. Surface Effects in Nuclear Matter: Macroscopic Description

The nuclear matter properties have been extensively studied for more than half a century. There exist quite a number of theoretical works devoted to different models of infinite nuclear matter, as well as finite nuclei. When discussing the different approaches, one can divide them into two groups that are microscopic and macroscopic approaches. At first glance, the microscopic approaches seem to be much more general than the macroscopic ones that deal only with the averaged values and can be obtained basically as the average of the microscopic theory. At the same time, the exact microscopic calculations are very challenging to perform, and the precise data on the micro-

scopic parameters are needed that makes it difficult for practical applications. During recent decades, the impressive progress has been achieved in the macroscopic description of nuclear matter [46, 77, 78]. A number of papers devoted to the thermodynamics of small systems or the hydrodynamics of nuclear matter appeared [4, 55, 57, 79, 80]. Therefore, the nuclear systems that consist of a number of nucleons that is neither very small nor very large seem to be a good object for being studied with the help of a combination of both macroscopic and microscopic approaches. The bright example of such a cooperation of the methods in nuclear physics is the liquid droplet model [81] introduced in the 1960s, which makes possible the description of the average properties of a saturated system such as a nucleus consisting of two components (neutrons and protons) with account for the boundary effects and the presence of a diffuse layer. In that case, the energy at equilibrium is given as

$$E = \left(-a_1 + J\bar{\delta}^2 + \frac{1}{2}K\bar{\epsilon}\bar{\delta}^2 + \frac{1}{2}M\bar{\delta}^4\right)A + \\ + a_2(1+2\bar{\epsilon})A^{\frac{2}{3}} + Q\tau^2 A^{\frac{2}{3}} + a_3 A^{\frac{1}{3}} + \\ + c_1\frac{Z^2}{A^{\frac{1}{3}}}\left(1 - \bar{\epsilon} + \frac{1}{2}\tau A^{-\frac{1}{3}}\right) - \\ - c_2 Z^2 A^{\frac{1}{3}} - c_3\frac{Z^2}{A} - c_4\frac{Z^{\frac{4}{3}}}{A^{\frac{1}{3}}} \qquad (7)$$

with

$$\frac{\rho}{\rho_0} = 1 - 3\epsilon, \\ \frac{\rho_n}{\rho} = \frac{1}{2}(1+\delta)\frac{r_0}{R} = A^{-\frac{1}{3}}, \qquad (8)$$

where J, K, M, Q, a_1, a_2, and a_3 are the coefficients evaluated from the observed averaged phenomenological inputs and some relations based on the different microscopic considerations, A is the nuclear mass number, and Z is the charge number. As a result, the liquid droplet model is able to provide a quite precise description of the properties of finite nuclei. As comes from the liquid droplet model in studying the curvature-correction term for the nuclear matter, one should keep in mind the connection between the surface and bulk properties of the matter [81, 82]. As shown in the droplet model, the coefficients in the term proportional to $A^{\frac{1}{3}}$ in the expansion of nuclear properties in terms of the fundamental dimensionless ratio $A^{-\frac{1}{3}}$ are related to the bulk properties of NM described by the terms proportional to A and $A^{\frac{2}{3}}$.

Corrections due to a curvature may play an important role, when studying light nuclei or processes, where surface terms are important. Particularly important are those corrections in the interpretation of multifragmentation experiments [80, 83–85], in which light nuclei necessarily appear. The exponential dependence of the yield of fragments on the surface tension makes this process sensitive to the curvature corrections [49, 86]. Other important phenomena that may be affected by changes in the surface tension due to curvature corrections are:

a) the appearance of the neck region in the fission processes and

b) the hydrodynamic instability of the structures formed in heavy ion experiments governed by surface effects [69, 87].

Quite a number of papers devoted to studies of the surface energy and the properties of surfaces in NM [88–90] have appeared. Furthermore, the dependence of the surface tension coefficient (and surface energy) on the surface curvature and its influence on different physical properties were also studied by various groups of researchers [82, 91]. Still for decades, it remains a controversial issue in mesoscopic thermodynamics [92–94].

The thermodynamic description of the curvature correction, originating from the difference between the equimolar surface and the surface of tension [95, 96], dates back to the 1940s. The Tolman length δ was originally introduced in [97] to describe the curvature dependence of the surface tension of a small liquid droplet. It was defined as a correction term in the surface tension σ of the liquid-vapour droplet in the isothermal case:

$$\sigma(R) = \sigma_\infty\left(1 - \frac{2\delta}{R} + ...\right), \qquad (9)$$

where R is the droplet radius equal to the radius of the surface tension [95, 96], and σ_∞ is the surface tension of a planar interface. Eq. (9) originates from the Gibbs–Tolman–Koenig–Buff's thermodynamic equation and the assumption that δ is independent of R for $\delta \ll R$ [98]. This physics should work not only for liquid droplets, but also for any system with curved interface of a non-negligible boundary layer [92]. This situation corresponds to nuclei and nuclear

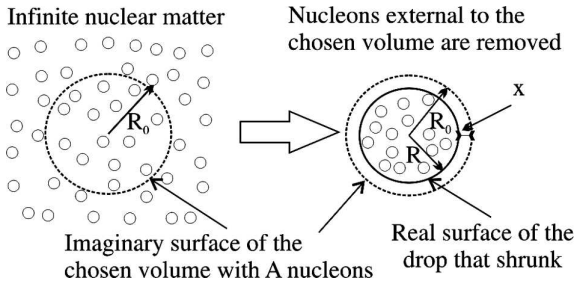

Fig. 12. Schematic picture of the *gedanken* experiment [99]

systems with a finite diffuse layer [77]. Based on that fact, a thermodynamic approach that links the EOS of NM with the curvature corrections to the surface tension coefficient has been introduced recently [99]. In this work, the analysis is based on the simple gedanken experiment. First, one should consider infinite nuclear matter (P_0, T = const) with the chosen spherical volume $V_0 = \frac{4}{3}\pi {R_0}^3$ in it consisting of A nucleons. If all the nucleons outside the chosen volume are removed, one gets a "nuclear droplet" that, due to the surface tension, shrinks to the volume $V = \frac{4}{3}\pi R^3$, where R is the final radius of the chosen volume (Fig. 12). This droplet remains in equilibrium. The analysis of changes in the surface size due to the shrinkage allows calculating the curvature correction to the surface tension coefficient from the EOS of NM. The Tolman length δ is calculated for different effective interactions (SLy6, SkM* and SV-min). The calculated results for δ in the case of, for example, the SV-min parametrization, appeared to be $\delta \sim -0.55$ fm that is close to the distance between the nucleons. That result correspond to the theoretical estimations based on the Gibbs–Tolman formalism. Therefore, the statistical thermodynamic approach can be useful in studies of the surface properties of nuclei.

4. Hadronic Matter and Quantum Liquids

Nowadays, there exist quite a lot of papers devoted to the application of classical results of the phase transition theory and the theory of ordinary liquids for hadronic matter and quantum liquids. That can be explained by the growing interest in and the understanding of the universality of critical phenomena in different media over a tremendous span of substances – from ultracold atoms to dense nuclear matter [100–103]. Calculations of the nucleation rate during the (de)confinement phase transition are subject for continuous debates with implications in the early Universe and relativistic HIC. The interest in this subject is triggered by the interpretation of the observed elliptic flow in heavy-ion collisions at RHIC [104–106] as a manifestation of the low shear viscosity of nuclear matter, and a subsequent realization [107] of the universality of this phenomenon, see also [108, 109]. Most remarkably, these studies penetrated [110–114] different neighboring fields of physics such as condensed matter and statistical mechanics and their interface with nuclear and astro-particle physics.

4.1. Quantum liquids

When applying the classical fluid thermodynamics to nuclear matter, quantum corrections become important as compared to the motion of atoms and molecules in ordinary liquids [115, 116]. There is an essential difference between nucleons, on the one hand, and nuclei, atoms, or molecules, on the other hand. In the latter case, the relevant energies – binding energies, exciting energies, *etc.* - are much smaller than the rest frame masses of the system or of the constituents. In the case of hadrons, they are of the same order as the mass of the system. Hence, the quantum effects are of importance.

The amount of quantum corrections to the classical theory can be quantified from the expansion in powers of the Planck constant h of the quantum statistical sum of a system of interacting particles. For the Helmholtz free energy, the following expression holds [115, 117], in which the first quantum correction is proportional to h^2:

$$F = F_{\text{class}} \left[1 + \left(\frac{\Lambda}{T^*} \right)^2 \omega \left(T^*, V^* \right) + ... \right]. \tag{10}$$

Here, F_{class} is the classical free energy, ω is some dimensionless function of the order of 1, and a new dimensionless parameter Λ is defined as

$$\Lambda = \frac{h}{\sigma \sqrt{m\varepsilon}}, \tag{11}$$

where m is the mass of the particle. Λ is called the de Boer parameter and describes the amount of quantum effects in statistical systems [115, 117].

The apparent similarity of the properties of different media suggests the use of the law of corresponding states (LCS) [115]. For real atoms and molecules, the intermolecular potential $\Phi(r)$ can be reduced, with

reasonable precision, to a product of the energy constant ε (the depth of the minimum in the particle interaction potential) and a function of the dimensionless variable $x = \frac{r}{\sigma}$,

$$\Phi(r) = \varepsilon\phi\,(x), \tag{12}$$

where σ is the position of the minimum. Then, by LCS, for a group of substances with a common potential $\phi(x)$, the universal functions for the pressure $p^* = p^*\,(T^*, V^*)$, energy $E^* = E^*\,(T^*, V^*)$, free energy $F^* = F^*\,(T^*, V^*)$, *etc.* should exist, where $T^* = \frac{kT}{\varepsilon}$ is the reduced temperature and $V^* = \frac{V}{\sigma^3}$ is the reduced volume. As a consequence, the thermodynamic properties of all the substances from a given group are similar in terms of a properly chosen scale. In view of the similarity of the nuclear forces to the van der Waals forces, see Fig. 11, LCS should work both in ordinary liquids and in nuclear matter.

Recently, it was suggested to extend the principle of corresponding states for ordinary liquids to the possible fluid-superfluid and conductor-superconductor transitions for a variety of systems, ranging from ^{3}He, ^{4}He, and superconducting electron fluids to nuclear matter. Such an extension is based on the description of the superfluidity phenomenon in terms of wave packets. Superfluidity assumes the appearance of phased waves (wave packets) of bosonic quantum particles due to the Bose condensation (Fig. 13).

As a consequence, it appeared to be possible to define the analogue of the de Boer parameter – dimensionless number BJEMS [118]

$$\text{BJEMS} = g\,l\,(mkT)^{1/2}\,/\hbar. \tag{13}$$

Analogously to the de Boer parameter, it takes the quantum effects into account. The difference is that it considers the exchange effects. Therefore, it might be used for the superfluid phase transitions. The parameter BJEMS is assumed to be of the same order of magnitude for all fluid-superfluid and conductor-superconductor transitions. This hypothesis is based on the general principles, rather than on the microscopic theory, and it appears to be correct for all the real Fermi and Bose systems from the same universality class.

4.2. Hadronic matter

Studies of the hadronic matter are an important part of the modern astrophysics and HIC physics. In the early Universe, a particular nucleation dynamics during the confinement can influence the inhomogeneities in the hadron distribution. Nowadays, the possibility for a number of colored objects such as quarks and gluons to escape the hadronization during the cooling of the Universe is intensively studied [119–121]. This requires the understanding of the surface properties of the formed quark "nuggets". Statistical thermodynamics can be quite helpful in the studies of those properties. In HIC, superheated hadron matter can produce extra entropy and might lead to observable consequences, detectable in the experiment. Earlier, there were the attempts to use statistical thermodynamic approaches for studying the hadron matter, confinement, phase transitions, and early evolution of the Universe [89, 122–124]. Within the suggested approach, some interesting results were obtained in the description of the expansion of the Universe during the early stages of its evolution. The behavior of the surface tension coefficient in the (de)confinement phase transitions was studied. The obtained results for a parton gas can be useful in the studies of the color-glass condensate that is discussed in the framework of the studies of relativistic HIC.

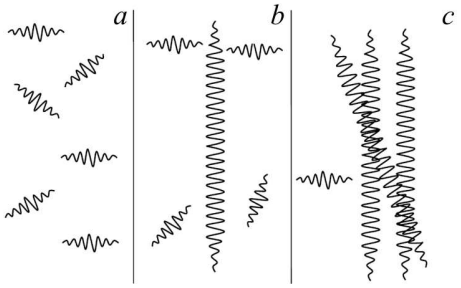

Fig. 13. Distribution of waves of particles: in a classical system (high temperatures) (a); exactly at the transition temperature (b); slightly below the transition point (c)

The similarity of the behavior of ordinary liquids and hadronic matter, as well as the existence of a number of interesting results obtained for hadronic matter from the statistical thermodynamic approaches, suggests the application of classical laws in high-energy physics.

5. Summary

Macroscopic theories well-developed for ordinary liquids have shown themselves to be successful in describing the average properties of nuclear sys-

tems. They work well for nuclear matter in combination with microscopic approaches naturally complementing each other. Hydrodynamic approaches developed for ordinary liquids are widely used in the studies of heavy ion collisions at different energies, as they explain well the observed phenomena, and their results can be easily compared to the calculations within transport theories. The thermodynamic description has shown to be fruitful for finite nuclei and intermediate-energy heavy ion collisions.

At the same time, statistical thermodynamics can be applied not only for ordinary liquids and nuclear matter, but also for studies of the properties of quark-gluon plasma. It has shown to be useful in understanding the behavior of quantum liquids in phase transitions.

Macroscopic theories can be used in constructing a proper equation of state of nuclear matter that is one of the long standing and desirable goals in nuclear physics. They can be used in the studies of the intermediate heavy-ion collisions, which are a window into the nuclear matter equation of state and can be treated as the analogue of the P-V-T studies in the physics of ordinary liquids.

Statistical thermodynamics and phase transition theory widely used in the physics of ordinary liquids work well for hadronic matter. They are quite fruitful in studying the (de)confinement phase transitions. Interesting results are found in the works devoted to the color glass condensate that is discussed in the context of relativistic heavy ion collisions. They can be useful in studies of the early evolution of the Universe.

As a summary, one can conclude that the approaches originally developed for ordinary liquids are widely used in the studies of hadronic matter and can give valuable results.

1. L.A. Bulavin and V.M. Sysoev, *Physics of phase transitions* (VPC "University of Kyiv", Kyiv, 2010).
2. L.A. Bulavin, D.A. Gavryushenko, and V.M. Sysoev, *Molecular Physics* (Znannya, Kyiv, 2006).
3. L.A. Bulavin and V.K. Tartakovskii, *Nuclear Physics* (Znannya, Kyiv, 2005).
4. D.H.E. Gross, *Microcanonical Thermodynamics: Phase Transitions in "Small" Systems*, (World Scientific, Singapore, 2001).
5. G.F. Bertsch and S. Das Gupta, Phys. Rep. **160**, 189 (1988).
6. M. Baldo and C. Maieron, J. Phys. G: Nucl. Part. Phys. **34**, R243 (2007).
7. Y. Abe, S. Ayik, P.-G. Reinhard, and E. Suraud, Phys. Rep. **275**, 49 (1996).
8. V. Baran, M. Colonna, V. Greco, and M. Di Toro, Phys. Rep. **410**, 335 (2005).
9. Bao-An Li, Lie-Wen Chen, and Che Ming Ko, Phys. Rep. **464**, 113 (2008).
10. V.A. Karnaukhov, Phys. Elem. Part. Atom. Nucl. **37**, 312 (2006).
11. S. Shlomo, J. Phys: Conf. Ser. **337**, 012014 (2012).
12. P.D. Stevenson and P.M. Goddard, in *Proceedings of the 31st International Workshop on Nuclear Theory*, edited by A. Georgieva and N. Minkov (Heron Press, Sofia, 2012).
13. K. Oyamatsu, I. Tanihata, Y. Sugahara, H. Toki, and K. Sumiyoshi, RIKEN Review **26**, 1 (2000).
14. M.B. Tsang, J.R. Stone, F. Camera, P. Danielewicz, S. Gandolfi, K. Hebeler, C.J. Horowitz, Jenny Lee, W.G. Lynch, Z. Kohley, R. Lemmon, P. Moller, T. Murakami, S. Riordan, X. Roca-Maza, F. Sammarruca, A.W. Steiner, I. Vidana, and S.J. Yennello, arXiv:12040466 [nucl-ex] (2012).
15. L.W. Chen, C.M. Ko, and B.A. Li, Phys. Rev. Lett. **94**, 032701 (2005).
16. L.W. Chen, C.M. Ko, and B.A. Li, Phys. Rev. C **76**, 054316 (2007).
17. T. Klahn, D. Blaschke, S. Typel, E.N.E. van Dalen, A. Faessler, C. Fuchs, T. Gaitanos, H. Grigorian, A. Ho, E.E. Kolomeitsev, M. C. Miller, G. Ropke, J. Trumper, D.N. Voskresensky, F. Weber, and H.H. Wolter, Phys. Rev. C **74**, 035802 (2006).
18. A.S. Botvina and I.N. Mishustin, Phys. At. Nucl. **71**, 1088 (2009).
19. S.R. Souza, B.V. Carlson, R. Donangelo, W.G. Lynch, A.W. Steiner, and M.B. Tsang, Phys. Rev. C **79**, 054602 (2009).
20. P. Danielewicz, R.A. Lacey, and W.G. Lynch, Science **298**, 1592 (2002).
21. J. Hufner, Phys. Rep. **125**, 129 (1985).
22. A.S. Botvina and I.N. Mishustin, Eur. Phys. J. **30**, 121 (2006).
23. K. Kwiatkowski, W.A. Friedman, L.W. Woo, V.E. Viola, E.C. Pollacco, C.Volant, and S.J. Yennello, Phys. Rev. C **49**, 1516 (1994).
24. J. Pan and S. Das Gupta, Phys. Rev. C **51**, 1384 (1995).
25. V.E. Viola, K. Kwiatkowski, J.B. Natowitz, and S.J. Yennello, Phys. Rev. Lett. **93**, 132701 (2004).
26. K.C. Chase and A.Z. Mekjian, Phys. Rev. Lett. **75**, 4732 (1995).
27. C. Fuchs and H.H. Wolter, Eur. Phys. J. A **30**, 5 (2006).
28. C.B. Das, S. Das Gupta, and A.Z. Mekjian, Phys. Rev. C **67**, 064607 (2003).
29. G. Chaudhuri and S. Das Gupta, Phys. Rev. C **80**, 044609 (2009).
30. P.J. Siemens, Nature **305**, 410 (1983).
31. M.R.D. Rodrigues, R. Wada, K. Hagel, M. Huang, Z. Chen, S. Kowalski, T. Keutgen, J. B. Natowitz, M. Barbui, A. Bonasera, K. Schmidt, J. Wang, L. Qin, T. Materna, and P.K. Sahu, J. Phys.: Conf. Ser. **312**, 082009 (2011).

32. B. Borderie and M.F. Rivet, Prog. Part. Nucl. Phys. **6**, 551 (2008).
33. N. Marie *et al.*, Phys. Rev. C **58**, 256 (1998).
34. H.R. Jaqaman and D.H.E. Gross, Nucl. Phys. A **524**, 321 (1991).
35. X. Campi, J. Phys. A **524**, 321 (1986).
36. M. Kleine Berkenbusch, W. Bauer, K. Dillman, S. Pratt, L. Beaulieu, K. Kwiatkowski, T. Lefort, W.C. Hsi, V.E. Viola, S.J. Yennello, R.G. Korteling, and H. Breuer, Phys. Rev. Lett. **88**, 22701 (2001).
37. A. Ono and J. Randrup, Eur. Phys. J. A **30**, 109 (2006).
38. J. Cugnon, Nucl. Phys. A **462**, 751 (1987).
39. J.P. Bondorf, H.T. Feldmeier, S. Garpman, and E.C. Halbert, Phys. Lett. B **65**, 217 (1976).
40. H. Stocker and W. Greiner, Phys. Rep. **137**, 277 (1986).
41. M.B. Tsang, R. Bougault, R. Charity, D. Durand, W.A. Friedman, F. Gulminelli, A. Le Fevre, Al.H. Raduta, Ad.R. Raduta, S. Souza, W. Trautmann, and R. Wada, Eur. Phys. J. A **30**, 129 (2006).
42. E. Bonnet and ALADIN Collaborations *et al.*, Phys. Rev. Lett. **103**, 072701 (2009).
43. A.S. Botvina, I.N. Mishustin, M. Begemann-Blaich, J. Hubele, G. Imme, I. Iori, P. Kreutz, G.J. Kunde, W.D. Kunze, V. Lindenstruth, U. Lynen, A. Moroni, W.F..J Muller, C.A. Ogilvie, J. Pochodzalla, G. Raciti, Th. Rubehn, H. Sann, A. Schttauf, W. Seidel, W. Trautmann, and A. Werner, Nucl. Phys. A **584**, 737 (1995).
44. X. Campi, H. Krivine, E. Plagnol, and N. Sator, Phys. Rev. C **67**, 044610 (2003).
45. G.F. Bertsch, Am. J. Phys. **72**, 983 (2004).
46. L.G. Moretto, J.B. Elliott, L. Phair, and P.T. Lake, J. of Phys. G **38**, 113101 (2011).
47. A.D. Panagiotou, M.W. Curtin, H. Toki, D.K. Scott, and P.J. Siemens, Phys. Rev. Lett. **52**, 496 (1984).
48. M.E. Fisher, Physics **3**, 255 (1967).
49. J. B. Elliott, P.T. Lake, L.G. Moretto, and L. Phair, Phys. Rev. C **87**, 054622 (2013).
50. E.A. Guggenheim, J. Chem. Phys. **13**, 253 (1945).
51. K.V. Cherevko, L.A. Bulavin, and V.M. Sysoev, Phys. Rev. C **84**, 044603 (2011).
52. V.P. Scripov, *Metastable Liquids* (Wiley, New York, 1974).
53. J.W. Cahn, J. Chem. Phys. **42**, 93 (1965).
54. V.G. Boyko, L.L. Jenkovszky, and V.M. Sysoev, EChAYa **22**, 675 (1991).
55. Ph.J. Siemens and J.O. Rasmussen, Phys. Rev. Lett. **42**(14), 880 (1979).
56. H. Stocker, R.Y. Cusson, J.A. Maruhn, and W. Greiner, Z. Phys. A **294**, 125 (1980).
57. H.G. Baumgardt, J.U. Schott, Y. Sakamoto, E. Schopper, H. Stocker, J. Hofmann, W. Scheid, and W. Greiner, Z. Phys. A **273**, 359 (1975).
58. G.Q. Li and R. Machleidt, Phys. Rev. C **48**, 1702 (1993).
59. T. Alm, G. Ropke, W. Bauer, F. Daffin, and M. Schmidt, Nucl. Phys. A **587**, 815 (1995).
60. Q. Li, Z. Li, S. Soff, M. Bleicher, and H. Stocker, J. Phys. G: Nucl. Part. Phys. **32**, 407 (2006).
61. L.W. Chen, V. Greco, C.M. Ko, and B.A. Li, Phys. Rev. C **68**, 014605 (2003).
62. H.H.K. Tang and Cheuk-Yin Wong, Phys. Rev. C **21**, 1846 (1980).
63. W. Bauer, G.F. Bertsch, and H. Schulz, Phys. Rev. Lett. **69**, 1888 (1992).
64. H. M. Xu, J.B. Natowitz, C.A. Gagliardi, R.E. Tribble, C.Y. Wong, and W.G. Lynch, Phys. Rev. C **48**, 933 (1993).
65. L.G. Moretto, K. Tso, and G.J. Wozniak, Phys. Rev. Lett. **78**, 824 (1997).
66. N.T.B. Stone, O. Bjarki, E.E. Gualtieri, S.A. Hannuschke, R. Lacey, J. Lauret, W.J. Llope, D.J. Magestro, R. Pak, A.M. Vander Molen, G.D. Westfall, and J. Yee, Phys. Rev. Lett. **78**, 2084 (1997).
67. R.F. Allen, J. Colloid Interface Sci. **51**, 350 (1975).
68. Cheuk-Yin Wong, Phys. Rev. Lett. **55**, 1973 (1985).
69. K. Cherevko, J. Su, L. Bulavin, V. Sysoev, and Feng-Shou Zhang, Phys. Rev. C **89**, 014618 (2014).
70. D. Bartolo, Ch. Josserand, and D. Bonn, Phys. Rev. Lett. **96**, 124501 (2006).
71. R. Rioboo, M. Marengo, and C. Tropea, Exp. Fluid. **33**, 112 (2002).
72. S.T. Thoroddsen and J. Sakakibara, Phys. Fluid. **10**, 1359 (1998).
73. Kuo-Long Pan, Ping-Chung Chou, and Yu-Jen Tseng, Phys. Rev. E **80**, 036301 (2009).
74. J. Eggers, M.A. Fontelos, Ch. Josserand, and S. Zaleski, Phys. Fluid. **22**, 062101 (2010).
75. A.V. Chizhov and A.A. Shmidt, J. Tech. Phys. **45**, 18 (2000).
76. I.V. Roisman, C. Planchette, E. Lorenceau, and G. Brenn, J. Fluid Mech. **690**, 512 (2012).
77. M. Brack, C. Guet, and H.-B. Hakansson, Phys. Rep. **123**, 275 (1985).
78. Ph. Chomaz, F. Gulminelli, and O. Juillet, Ann. Phys. **320**, 135 (2005).
79. C.-Y. Wong, Phys. Rev. C **78**, 054902 (2008).
80. Ph. Chomaz, M. Colonna, and J. Randrup, Phys. Rep. **389**, 263 (2004).
81. W.D. Myers and W.J. Swiatecki, Ann. Phys. **55**, 395 (1969).
82. L.G. Moretto, J.B. Elliott, P.T. Lake, and L. Phair, AIP Conf. Proc. **1491**, 75 (2012).
83. D.H.E. Gross, Rep. Prog. Phys **53**, 605 (1990).
84. Feng-Shou Zhang, Zeit. für Phys. A **356**, 163 (1996).
85. F.-S. Zhang and L.X. Ge, *Nuclear Multifragmentation* (Science Press, Beijing, 1998).
86. Jan Toke, Jun Lu, and W. Udo Schroder, Phys. Rev. C **67**, 034609 (2003).
87. U. Brosa and S. Grossmann, Z. Phys. A **310**, 177 (1983).
88. D.G. Ravenhall, C.J. Pethick, and J.M. Lattimer, Nucl. Phys. A **407**, 571 (1983).
89. V.G. Boyko, L.L. Jenkovszky, and V.M. Sysoev, Zeit. Phys. C **45**, 607 (1990).
90. L.L. Jenkovszky, B. Kampfer, and V.M. Sysoev, Sov. J. Nucl. Phys. **57**, 1507 (1994).
91. K. Pomorski and J. Dudek, Phys. Rev. C **67**, 044316 (2003).
92. M.A. Anisimov, Phys. Rev. Lett. **98**, 035702 (2007).
93. E.M. Blokhius and J. Kuipers, J. Chem. Phys. **124**, 074701 (2006).

94. V.M. Kolomietz, S.V. Lukyanov, and A.I. Sanzhur, Phys. Rev. C **86**, 024304 (2012).
95. J.S. Rowlinson and B. Widom, *Molecular Theory of Capillarity* (Clarendon, Oxford, 1982).
96. J.S. Rowlinson, J. Phys.: Condens. Matter **6**, A1 (1994).
97. R.C. Tolman, J. Chem. Phys. **17**, 333 (1949).
98. S. Ono and S. Kondo, *Molecular Theory of Surface Tension in Liquids* (Springer, Berlin, 1960).
99. K.V. Cherevko, L.A. Bulavin, L.L. Jenkovszky, V.M. Sysoev, and Feng-Shou Zhang, Phys. Rev. C **90**, 017303 (2014).
100. G.S. Denicol, T. Kodama, and T. Koide, arXiv:1002.2394 [nucl-th].
101. S. Pal, arXiv:1001.1585[nucl-th].
102. P. Bozek, arXiv:0911.2397[nucl-th].
103. T. Schafer and D. Teaney, Rep. Progr. Phys. **72**, 126001 (2009).
104. I. Arsene *et al.* (BRAHMS Collaboration), Nucl. Phys. A **757**, 1 (2005).
105. B.B. Back *et al.* (PHOBOS Collaboration), Nucl. Phys. A **757**, 28 (2005).
106. K. Adcox *et al.* (PHENIX Collaboration), Nucl. Phys. A **757**, 184 (2005).
107. L.P. Csernai, J.I. Kapusta, and L.D. McLerran, Phys. Rev. Lett. **97**, 152303 (2006).
108. M.I. Gorenstein, M. Hauer, and O.N. Moroz, Phys. Rev. C **77**, 024911 (2008).
109. E. Khan, arXiv:0905.3335[nucl-th].
110. K. Maeda, G. Baym, and T. Hatsuda, arXiv: 0904.4372 [cond-mat.quant.gas].
111. Renxin Xu, arXiv:0912.0349[astro-ph.HE].
112. E. Taylor and M. Randera, arXiv:1002.0869[cond-mat.quant-gas].
113. T. Koide, E. Nakano, and T. Kodama, arXiv: 0901.3707 [hep-ph].
114. G.G.N. Angilella *et al.*, arXiv:0901.265[cond-mat.stat-mech].
115. I.Z. Fisher, *Statistical Theory of Liquids* (Univ. of Chicago Press, Chicago, 1964).
116. J. De Boer, Physica **14**, 139 (1948).
117. L.D. Landau and E.M. Lifshitz, *Course of Theoretical Physics*, Vol. 5 (Pergamon, Oxford, 1980).
118. L.A. Bulavin, L.L. Jenkovszky, V.K. Magas, V.M. Sysoev, and K.V. Cherevko, in *Proceedings of the 2-nd International Conference on Current Problems in Nuclear Physics and Atomic Energy*, Vol. 1, P. 201 (Institute for Nuclear Research of NASU, Kyiv, 2008).
119. E. Witten, Phys. Rev. D **30**, 272 (1984).
120. D. Chandra and A. Goyal, Phys. Rev. D **62**, 063505 (2000).
121. M. Brilenkov, M. Eingorn, L. Jenkovszky, and A. Zhuk, Eur. Phys. J. C **74**, 3011 (2014).
122. L.L. Jenkovszky, B. Kampfer, and V.M. Sysoev, Z. Phys. C **48**, 147 (1990).
123. V.G. Boyko, L.L. Jenkovszky, B. Kampfer, and V.M. Sysoev, Astron. Nachrichten. **311**, 265 (1990).
124. L.A. Bulavin, L.L. Jenkovszky, S.M. Troshin, and N.E. Tyurin, EChAYa **41**, 924 (2010).

Received 22.05.15

К.В. Черевко, Л.Л. Єнковський,
В.М. Сисоев, Фен-Шоу Жанг

ЗАГАЛЬНИЙ ПІДХІД
ДЛЯ ОПИСУ КЛАСИЧНИХ РІДИННИХ
СИСТЕМ І ЯДЕРНОЇ МАТЕРІЇ

Р е з ю м е

В роботі робиться спроба короткого огляду можливостей застосування статистичної термодинаміки при вивченні адронної матерії. Розглядається можливість застосування гідродинаміки для опису формування різних топологічних структур в лобових зіткненнях важких іонів за малих енергій. Показано, що такий підхід дозволяє отримати аналітичний опис кожної стадії процесу та визначити властивості ядерної матерії (поверхневий натяг, стистливість та ін.) з аналізу властивостей утворених фрагментів. Розглядаються переваги термодинамічного аналізу фазових траєкторій систем, що утворюються в зіткненнях важких іонів. Розглядається можливість використання статистичної термодинаміки для визначення поправок до коефіцієнту поверхневого натягу, викликаних кривизною поверхні, з рівняння стану ядерної матерії. Розглянуто приклади застосування статистичної термодинаміки в дослідженнях адронної матерії та квантових рідин.